

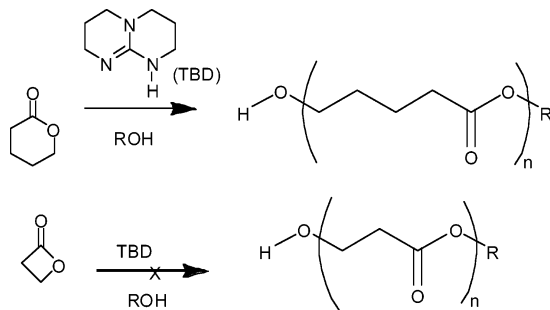
The Mechanism of TBD-Catalyzed Ring-Opening Polymerization of Cyclic Esters

Luis Simón and Jonathan M. Goodman*

Unilever Centre for Molecular Science Informatics, Department of Chemistry, University of Cambridge,
Lensfield Road, Cambridge CB2 1EW, United Kingdom

j.m.goodman@ch.cam.ac.uk

Received September 24, 2007



Triazabicyclodecene (TBD) has recently been shown to be an effective organocatalyst for the ring-opening polymerization (ROP) of cyclic esters. Using DFT methods, we have studied possible mechanisms of this reaction. Our studies explain not only the narrow polydispersity index (PDI) observed in the ROP of six-membered ring lactones, but also the surprising failure of the ROP for the more reactive butyrolactone.

Introduction

Strong amidine bases, such as DBN (1,5-diazabicyclo[4.3.0]-non-5-ene), DBU (1,8-diazabicyclo[5.4.0]undec-7-ene), TMG (tetramethyl guanidine), TBD (1,5,7-triazabicyclo[4.4.0]dec-5-ene), and MTBD (7-methyl-TBD), have been shown to promote many reactions, including elimination reactions, to form olefins,¹ Wittig reactions,^{2,3} and the additions of dialkyl phosphates or nitroalkanes to unsaturated systems.⁴ In addition to their usual role as general base catalysts, amidines, such as DBU, have been found to catalyze reactions acting as a nucleophile.⁵

These bases have also been used as catalysts in Michael reactions of malonates to α,β unsaturated ketenes, nitriles, and nitro groups,⁶ Strecker reactions,⁷ and transesterification reactions.⁸ In these reactions, TBD shows a higher catalytic activity

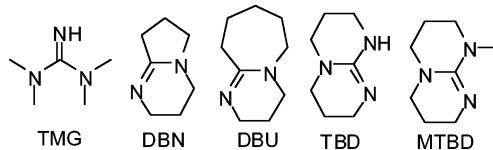


FIGURE 1. Structure of amidine bases.

when compared to the other amidine bases. Recently, TBD has been reported by Waymouth, Hedrick, and co-workers as promoting ring-opening polymerization (ROP) of the cyclic esters δ -valerolactone, ϵ -caprolactone, and L-lactide (see structures in Scheme 1) leading to polymers with a narrow polydispersity.⁹ This paper reports that TBD reacts with vinyl acetate to form *N*-acetyl-TBD, which reacts with an excess of benzyl alcohol to form benzyl acetate. This observation suggested to the authors the bifunctional nucleophilic mechanism shown in

* Address correspondence to this author. Phone: +44 (0)1223 336434. Fax: +44 (0)1223 763076.

(1) Oediger, H.; Moller, F.; Eiter, K. *Synthesis* **1972**, 591–598.

(2) Simoni, D.; Rondanin, R.; Morini, M.; Baruchello, R.; Invidiata, F. P. *Org. Lett.* **2000**, 2, 3765–3768.

(3) Edwards, M. F.; Williams, J. M. *Angew. Chem., Int. Ed.* **2002**, 41, 4740–4743.

(4) Simoni, D.; Rondanin, R.; Morini, M.; Baruchello, R.; Invidiata, F. P. *Tetrahedron Lett.* **2000**, 41, 1607–1610.

(5) Ghosh, N. *Synlett* **2004**, 3, 574–575.

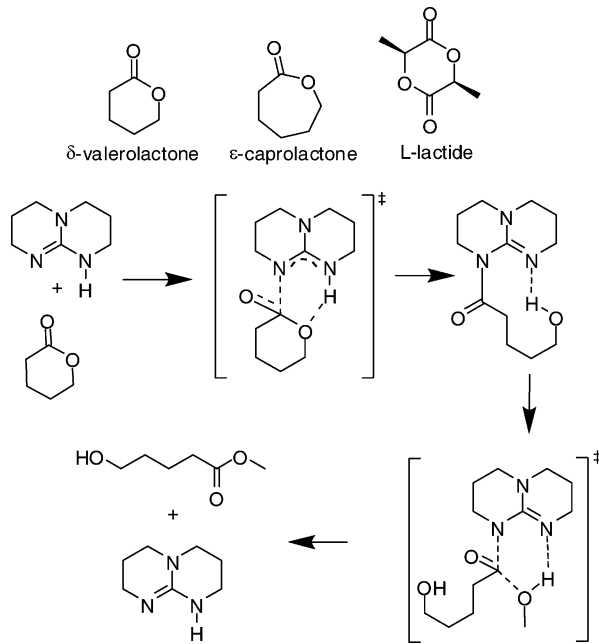
(6) Ye, W.; Xu, J.; Tan, C.-T.; Tan, C.-H. *Tetrahedron Lett.* **2005**, 46, 6875–6878.

(7) Corey, E. J.; Grogan, M. J. *Org. Lett.* **1999**, 1, 157.

(8) Schuchardt, U.; Vargas, R. M.; Gelbard, G. *J. Mol. Catal. A: Chem.* **1995**, 99, 65–70.

(9) Pratt, R. C.; Lohmeijer, B. G. G.; Long, D. A.; Waymouth, R. M.; Hedrick, J. L. *J. Am. Chem. Soc.* **2006**, 128, 4556–4557.

SCHEME 1. Structure of Substrates Used in ROP by Hedrick and the Proposed Mechanism for δ -Valerolactone Polymerization



Scheme 1 for δ -valerolactone. In this mechanism, nucleophilic attack of the amidine imine nitrogen to the ester carbonyl generates an activated intermediate. This intermediate then reacts with an incoming alcohol molecule, liberating the polymerized ester. The fact that the *N*-methyl derivative of TBD (MTBD) is much less active than TBD for this reaction is consistent with the mechanism.

Surprisingly, however, the TBD-catalyzed reaction was unsuccessful when polymerization was attempted with the more reactive butyrolactone. It is not clear from the reaction sequence in Scheme 1 why this change in behavior should occur when the lactone starting material is replaced with a more reactive analogue.

The low polydispersity index (PDI) observed for this reaction suggests that the process is a living polymerization. For such processes, chain termination, chain breaking, and chain transfer reactions are absent.¹⁰ The polymerization is started by addition of a small quantity of an initiator, 4-pyrenebutanol. The growing polymer chain terminates with a hydroxyl group, which is not too susceptible to side reactions. A chain transfer reaction, where the terminal alcohol attacks an ester in the middle of another polymer chain, is mechanistically reasonable. The low PDI is evidence, however, that this process is not competitive with chain extension.

Williams and co-workers¹¹ have studied the mechanism of ROP of ϵ -caprolactone catalyzed by methanol molecules. These authors studied two mechanistic possibilities: a concerted and a stepwise mechanism (Scheme 3). The first assumes that intermolecular C–O bond formation and intramolecular C–O bond breaking occurs simultaneously, and two additional methanol molecules assist the proton transfer from the nucleophile to the leaving group. The second, stepwise, mechanism

(10) Nicholson, J. *The Chemistry of Polymers*, 3rd ed.; RSC publishing: Cambridge, UK, 2006.

(11) Buis, N.; French, S. A.; Ruggiero, G. D.; Stengel, B.; Tulloch, A. D.; Williams, I. H. *J. Chem. Theory Comput.* **2007**, 3, 146–155.

is found to be more favorable. In this mechanism, transition state leads to a tetrahedral intermediate in which one of the methanol molecules is protonated. Because TBD is a stronger base than methanol, it is reasonable to suggest that this kind of mechanism may occur in the TBD-catalyzed ROP.

Following the Williams analysis of methanol-catalyzed ROP, an alternative mechanistic scheme for the TBD-catalyzed ROP reaction may be proposed. This is shown as Mechanism B in Scheme 4. The Waymouth and Hedrick proposal is Mechanism A in the same scheme. In this study, we use computational methods to analyze possible mechanisms for the process, and suggest explanations for all of the experimental observations.

Results and Discussion

To ensure that the calculations were computationally accessible, we have used methyl acetate and methanol as models for the growing fragment. These models are free of ring tension and, in the case of the methyl acetate, will probably show a similar conformation as the growing chain at the reaction center. The propagation reaction (Scheme 2) is modeled as methanolysis of valerolactone, and the chain transfer reaction between two polymer fragments (Scheme 2) is represented by the methanolysis of methyl acetate. All these processes are illustrated in Figure 2.

DFT calculations have been performed with Jaguar.¹² For optimizations and transition state searches, the hybrid B3LYP¹³ functional has been used with the 6-31+G*^{14–16} basis set, augmented with polarization and diffuse functions in transferable methanol and TBD protons. Vibrational contributions to zero-point energy and Gibbs free energy were calculated at this level of theory by using the harmonic approximation. For each optimized structure, single-point energy was calculated by using the DFT B3LYP functional and the 6-311++G**^{14–16} basis set, and this energy was added to the zero-point energy correction and the free Gibbs energy correction calculated at the same level of theory used in the optimization. For both geometry optimization and single-point energy calculation, solvent (CH₂Cl₂) was implicitly included, using a self-consistent reaction-field method as implemented in Jaguar^{17,18} (solvent dielectric constant = 9.1; probe radius = 2.3336912).

We have investigated both the nucleophilic catalytic mechanism originally proposed (Scheme 4, Mechanism A) and the acid–base catalytic mechanism (Scheme 4, Mechanism B), in which amidine basic nitrogen establish a H-bond with methanol, enhancing its nucleophilicity. This activated methanol reacts with an ester molecule which carbonyl oxygen is H-bonded to the TBD N-H group. In the transition state, both C–O bond formation and proton transfer occurs simultaneously, yielding a tetrahedral intermediate stabilized by H-bonding to the TBD catalyst. The tetrahedral intermediate undergoes an internal

(12) Jaguar, version 6.5, New York, 2006.

(13) Becke, A. D. *J. Chem. Phys.* **1993**, 104, 5648–5652.

(14) Clark, T.; Chandrasekhar, J.; Schleyer, P. v. R. *J. Comput. Chem.* **1983**, 4, 294–301.

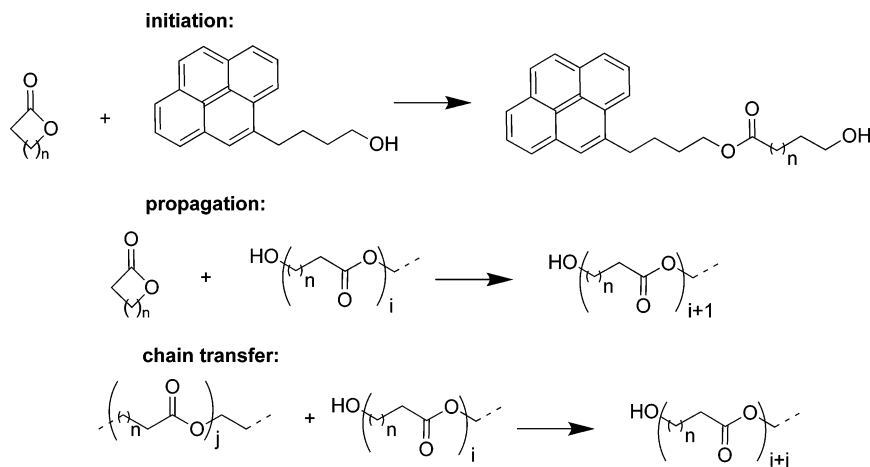
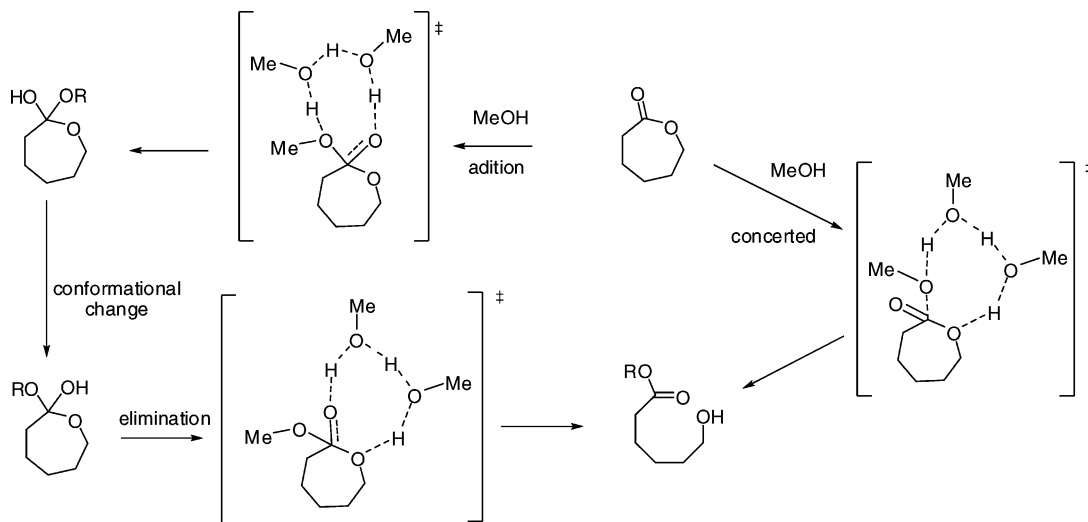
(15) Krishnam, R.; Binkley, J. S.; Seeger, R.; Pople, J. A. *J. Chem. Phys.* **1980**, 72, 650–654.

(16) Gill, P. M. W.; Johnson, B. G.; Pople, J. A.; Frisch, M. J. *Chem. Phys. Lett.* **1992**, 197, 499–505.

(17) Tannor, D. J.; Marten, B.; Murphy, R.; Friesner, R. A.; Sitkoff, D.; Nicholls, A.; Ringnalda, M.; Goddard, W. A., III; Honig, B. *J. Am. Chem. Soc.* **1994**, 116, 11875–11882.

(18) Marten, B.; Kim, K.; Cortis, C.; Friesner, R. A.; Murphy, R. B.; Ringnalda, M. N.; Sitkoff, D.; Honig, B. *J. Phys. Chem.* **1996**, 100, 11775–11788.

SCHEME 2. Initiation, Propagation, and Chain Transfer Reactions in the ROP of Lactones

SCHEME 3. Williams's Study of the Mechanism of ROP for ϵ -Caprolactone Catalyzed by Methanol¹¹

rotation, and the new intermediate reacts through a similar concerted proton transfer and elimination transition state structure to yield products. A similar mechanism, in which a guanidine is active in a double proton-transfer reaction, has previously been proposed by Han and co-workers in the guanidine-catalyzed Strecker reaction.¹⁹ Both Mechanism A and Mechanism B require a proton on the TBD nitrogen, and so MTBD should not be a catalyst, as is observed.

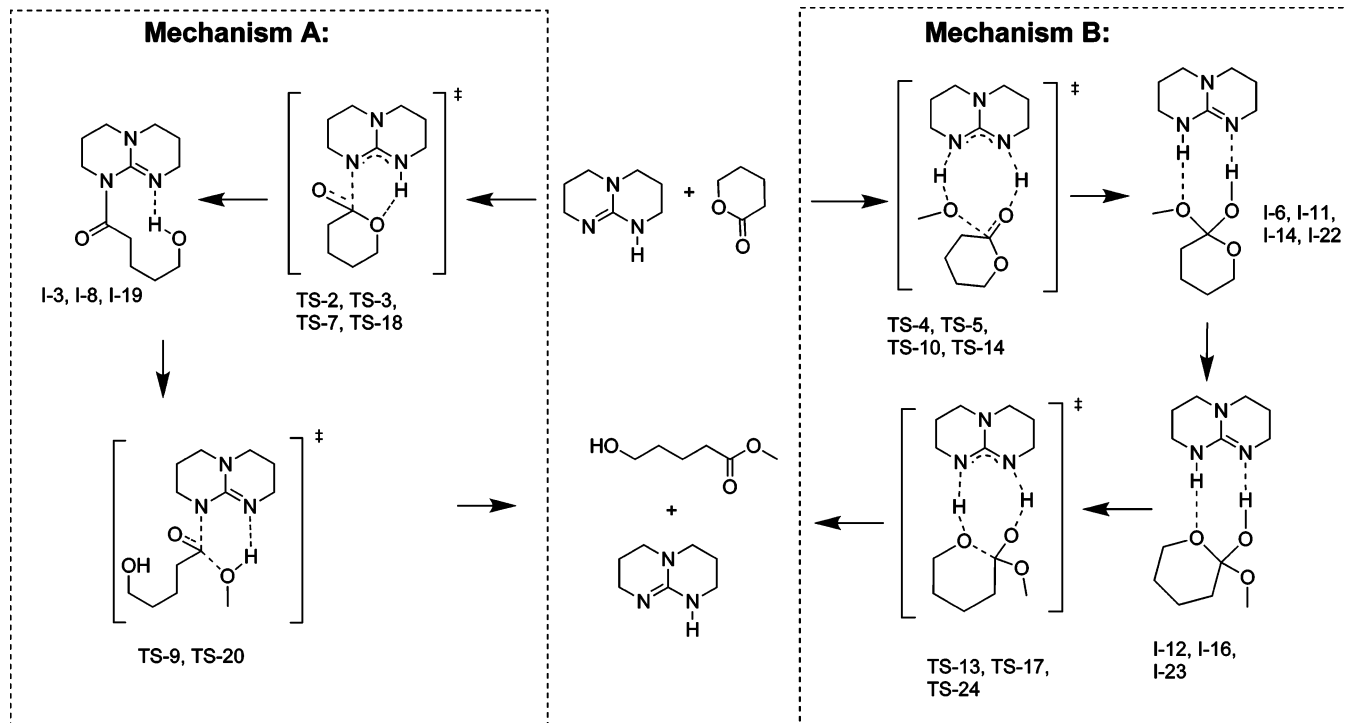
Our studies focused on the reactions of both valerolactone and methyl acetate. For the methyl acetate reaction (Figure 3), different transition states can be obtained starting from the *E* or the *Z* conformations. The figure traces the reaction paths half way along the reaction coordinate. Since the reaction is the transesterification of methyl acetate with methanol, the second half of the reaction coordinate follows the same intermediates and barriers as the first half. The intermediate I-6 must undergo an internal rotation to switch the hydrogen bond from one methoxy oxygen to the other. The very flat potential energy surface for this process meant that searches for the transition structure for this process were unsuccessful, but indicated that the barrier for the rotation would be low. It is clear that the transition state structures corresponding to the acid–base

catalytic pathway (Mechanism B) are energetically favored over the ones corresponding to the nucleophilic catalytic reaction (Mechanism A), as there is more than 7 kcal mol⁻¹ difference in free Gibbs energy barriers. Since the alcohol (either initiator or growing chain) concentration will appear in the kinetic equation for Mechanism B, its value has to be taken into account when comparing the mechanisms. At room temperature, a 7 kcal mol⁻¹ difference implies that Mechanism A will only predominate at alcohol concentrations below 0.01 mM. The initiator is used in a greater concentration (7 mM).

The same holds, with even bigger free Gibbs energy barriers differences, in the case of the δ -valerolactone reaction (Figure 4). In this process, it was necessary to consider different cyclohexane ring conformations in the acid–base catalytic reaction (Mechanism A). Once again, it has not been possible to obtain transition state structures for internal rotation connecting intermediates I-11 and I-12 or I-15 and I-16, but the barriers for these processes should be low. The preference of TS-14 (axial attack of methanol) over TS-10 (equatorial attack of methanol) can be explained by considering a stereoelectronic effect: In TS-14 nucleophilic attack is antiperiplanar to non-bonding lone electron pairs of adjacent oxygen lactone atoms.^{20,21} In the opening of the cyclic tetrahedral intermediates

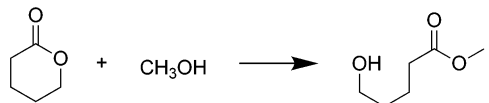
(19) Li, J.; Jiang, W.-Y.; Han, K.-L.; He, G.-Z.; Li, C. *J. Org. Chem.* **2003**, *68*, 8786–8789.

(20) Deslongchamps, P. *Tetrahedron* **1975**, *31*, 2463–2490.

SCHEME 4. Nucleophilic Catalytic Mechanism (A) and Acid–Base Catalytic Mechanism (B) of TBD in ROP of Lactones^a

^a Several conformations were found for most of intermediates and transition structures, and the labels of all the relevant conformations are listed by each structure.

model for propagation reaction:



model for chain transfer reaction:



FIGURE 2. Model reactions used in computational studies.

TS-13 is preferred over TS-17, because the lone pairs anti-periplanar to C–O bonds persist in the acyclic product²¹ (Figure 5). This is a late transition state, as indicated by the long distance between ester carbon and oxygen leaving group, and so the geometry is product-like.

Our calculations predict a smaller reaction barrier for the δ -valerolactone methanolysis than for methyl acetate methanolysis. For the whole reaction path, there is an overall difference in the Gibbs free energy barrier of about 4.5 kcal mol⁻¹. As a result, the reaction with the acyclic substrate, which leads to an uncontrolled polymer growing (Figure 2, chain transfer), is slower than the reaction with the cyclic substrate (Figure 2, propagation), in which the polymer increases its size in one monomer unit for every reaction step. This contributes to the narrow polydispersity observed in the ROP. This is also the case if only nucleophilic catalysis (Mechanism A) is considered, but the energy difference is smaller (2 kcal mol⁻¹). The origin of this effect could be the additional stabilization (3.3 kcal mol⁻¹) of the acyclic ester when it adopts the Z conformation. In fact, the reaction barrier from the E confor-

tion of the acyclic ester to the transition state structure (28.3 kcal mol⁻¹) is similar to the activation free energy in the δ -valerolactone reaction.

Therefore, the higher reactivity of cyclic esters can be explained by the destabilization of the E conformation in the starting material, and especially that this destabilization is not present in the corresponding transition state structure, even though early transition states, which contain structural features of the starting materials, have been obtained. The additional stability of the Z conformation in esters has been attributed to smaller steric effects, delocalization of the n-electron pair on the ether oxygen to occupy an antibonding C–O σ -bond of the carbonyl group, and favorable orientation of bond dipoles.^{22–25} Our calculations of the relative stabilities and dipole moments of esters are similar to those previously reported,^{24–25} even though the level of theories used are different.

Second-order perturbation theory analysis of Fock matrix using NBO orbitals²⁶ allows us to quantify the energy associated with n– σ^* delocalization as 8.3 kcal mol⁻¹ in the Z conformation of methyl acetate calculated at the level of theory described previously. This contrasts with the negligible 0.9 kcal mol⁻¹ obtained in the E conformation, since this conformation does not have the right geometry to allow overlapping of the orbitals. Despite this stabilization in the methyl acetate, similar analysis for the TS-5 structure yields 8.4 kcal mol⁻¹ stabilization (in

(22) Huisgen, R.; Ott, H. *Tetrahedron* **1959**, *6*, 253–267.

(23) Wiberg, K. B.; Laidig, K. E. *J. Am. Chem. Soc.* **1987**, *109*, 5935–5943.

(24) Wiberg, K. B.; Wong, M. W. *J. Am. Chem. Soc.* **1993**, *115*, 1078–1084.

(25) Evanseck, J. D.; Houk, K. N.; Briggs, J. M.; Jorgensen, W. L. *J. Am. Chem. Soc.* **1994**, *116*, 10630–10638.

(26) Glendening, E. D.; Weinhold, F. J. *Comput. Chem.* **1998**, *19*, 593–609.

(21) Perrin, C. L. *Acc. Chem. Res.* **2002**, *35*, 28–34.

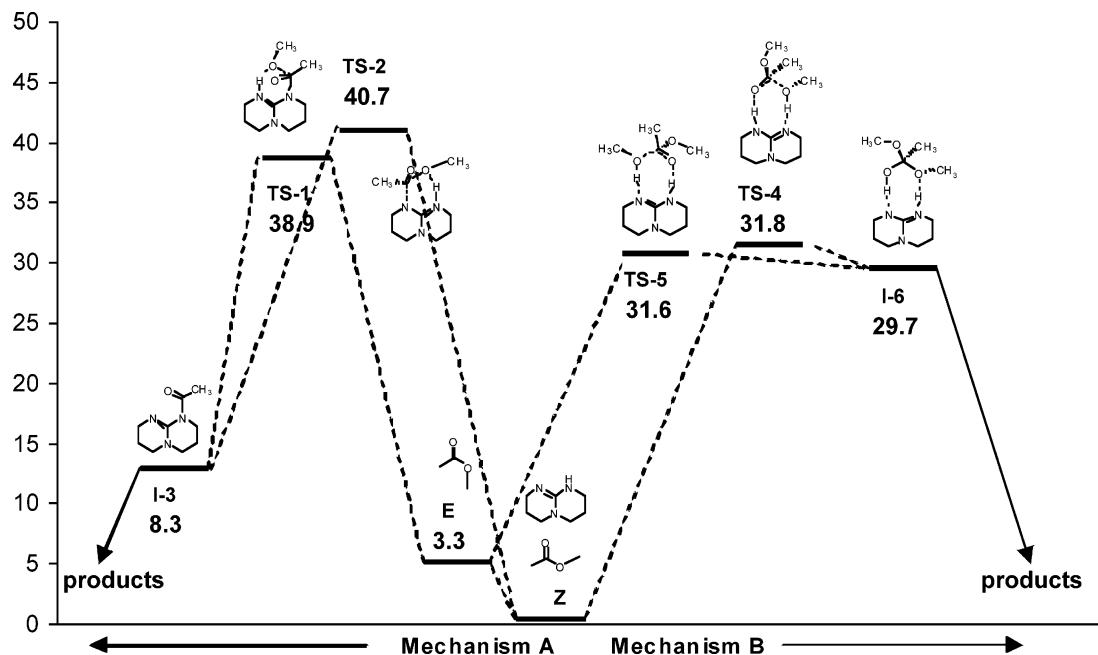


FIGURE 3. Energy profile and structures obtained for the reaction between methyl acetate and methanol.

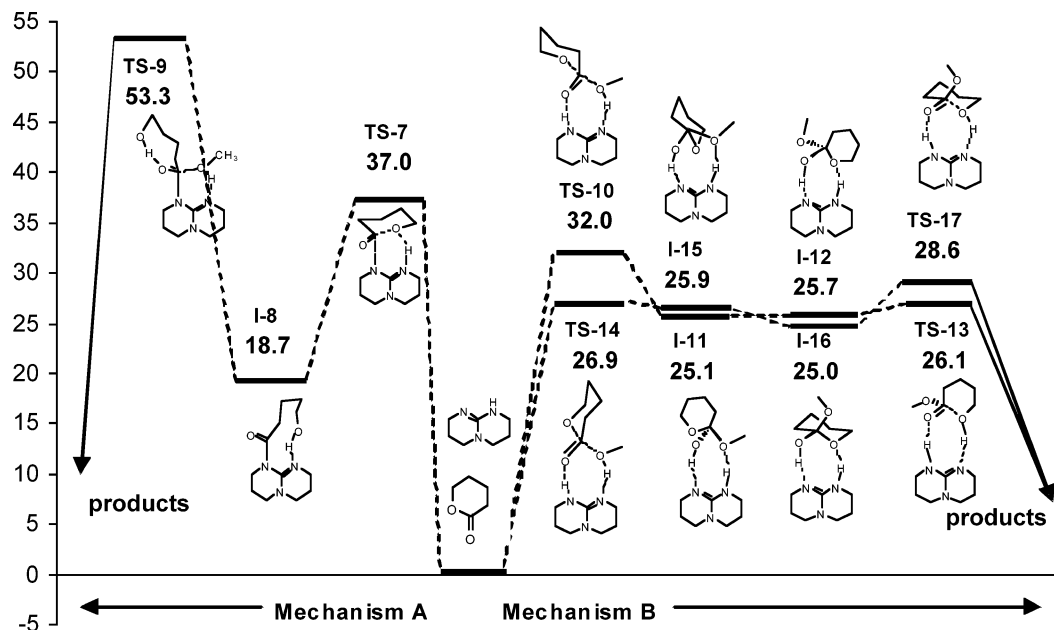


FIGURE 4. Energy profile and structures obtained for the reaction between δ -valerolactone and methanol.

agreement with the early character of the transition state). Thus, delocalization cannot explain the different energy barriers obtained for the reaction of *Z* and *E* conformation. Similarly, steric interactions between methyl groups in *E*-methyl acetate should be similar in the TS-5 structure, as shown by similar C–C distances (2.847 Å in *E*-methyl acetate, 2.865 Å in TS-5).

Unfavorable orientation of bond dipoles reinforces the molecular dipole moment. The dipole moment for the *Z* conformation (6.54 D) is bigger than the dipole moment of the *E* conformation (2.58 D). In the transition state structures these bond dipoles also interact with the catalyst. Molecular dipole moments calculated for TS-4 (9.77 D) and TS-5 (13.12 D) structures show the opposite tendency. More unfavorable bond

dipole interactions in *Z*-like TS-5 compensate for the more favorable steric and delocalization effects. As a corollary, the use of more polar solvents, which would stabilize molecular dipole moments, will decrease the reactivity difference between acyclic esters and lactones and increase the PDI in the product.

The ROP of β -butyrolactone was unsuccessful.⁹ No polymer was obtained at 298 K and only oligomer formation was observed on heating to 323 K. This contrasts to the high conversions observed at room temperature for δ -valerolactone, ϵ -caprolactone, and L-lactide, even though these substrates are less reactive to transesterification than the strained β -butyrolactone. The mechanistic studies should account for these unusual results, so the methanolysis catalyzed by TBD of this reactant was investigated considering both acid–base and

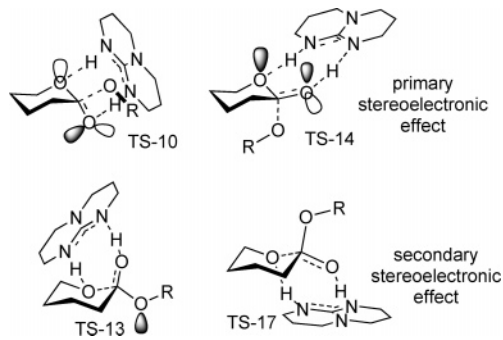


FIGURE 5. A primary stereoelectronic effect favors TS-14 over TS-10. Orbital lobes antiperiplanar to the nucleophilic group are shaded. A secondary stereoelectronic effect is responsible for higher stability of TS-13 over TS-17. The antiperiplanar lone pair interaction that persists in the product is indicated on TS-13.

nucleophilic catalytic pathways. The results for this study are shown in Figure 6. Unlike the previous reactions, Gibbs free energy barriers for nucleophilic addition of TBD (Mechanism A) and methanol acid–base addition (Mechanism B) are similar (1 kcal mol⁻¹ in favor of methanol addition, comparing TS-18 and TS-21). Because the concentration of hydroxyl groups under the experimental conditions is small (the concentration of the initiator, 4-pyrenebutanol, is only 0.007 M), and this concentration appears in the kinetic equation for Mechanism B, the formation of the acyl-TBD intermediate should be the fastest process. This acyl-TBD intermediate is particularly stable compared with the butyrolactone, probably due to the strain of the four-membered ring: only 1.3 kcal mol⁻¹ less stable than the starting materials. The calculations suggest that the intermediate is generated in a reversible process. However, only 0.1% of TBD is added relative to the monomer in the experimental conditions, and so most of the catalyst is likely to be trapped as this unproductive compound. This analysis explains why the ROP reaction with β -butyrolactone is unsuccessful.

Conclusions

In summary, we have studied the catalytic mechanism of ring-opening polymerization (ROP) of lactones in the presence of 1,5,7-triazabicyclo[4.4.0]dec-5-ene (TBD). We conclude that the ROP reaction has a choice of Mechanism A, through an amide-like intermediate, or Mechanism B, through lactone intermediates. Despite the small concentration of initiator used in reaction conditions, Mechanism B is preferred for the reaction of δ -valerolactone. This mechanism accounts for the experimental results in Waymouth and Hedrick's paper:

(i) The use of β -butyrolactone might be expected to speed the reaction up, because of the greater strain in the starting material, and so the greater energy released in the polymerization process. However, the strain in the starting material favors Mechanism A over Mechanism B, and so an amide-like intermediate is formed. The energy barrier to form the product from this intermediate is insurmountable, and so the reaction cannot go on. The equilibrium between the intermediate and the starting materials favors the intermediate, because of the excess of monomer. Consequently, the catalyst is trapped, and the reaction should not proceed, in line with the experimental observations.

(ii) Higher reactivity of cyclic lactones with respect to acyclic esters (in the Z conformation) contributes to the low PDI observed. The lower reaction barriers obtained for lactones are a consequence of the more favorable dipole-charge interactions in the E transition state and the higher stability of acyclic esters in the Z conformation. Additionally, the reactions show non-negligible reaction barriers, indicating that ROP is not diffusion controlled, but a relatively slow process, which is also consistent with a living polymerization process. As a consequence, every polymer chain grows at about the same rate, and is not affected by very rapid fluctuations in the local concentration of the cyclic ester.

(iii) In the original paper, Mechanism A is proposed based on the identification of the acyl intermediate I-8 as the product of the reaction of TBD with vinyl acetate. Nevertheless, this reaction takes place in the absence of any alcohol, so Mechanism

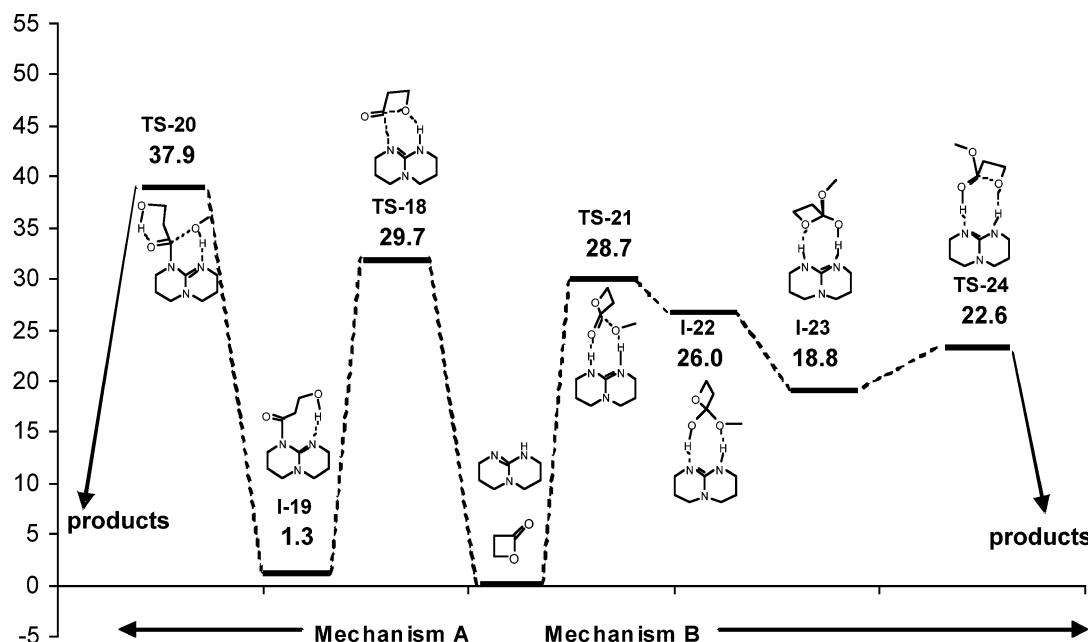


FIGURE 6. Energy profile and structures obtained for the reaction between β -butyrolactone and methanol.

B is impossible under the conditions of this test. Moreover, our calculations suggest that for highly reactive esters, like vinyl acetate, this intermediate shows an increased stability. This is not the case for δ -valerolactone, so the feasibility of this intermediate should not be taken as experimental evidence in favor of Mechanism A for this substrate. The subsequent conversion to benzyl acetate occurs with 5 equiv of the benzyl alcohol. This is rather different conditions to the low concentration of free alcohol, which is likely to be present under ROP conditions.

(iv) The reaction rate is not increased with more polar solvents as THF and DMF. This is in agreement with the non-charge-separated mechanisms proposed here.

Acknowledgment. This research was supported by a Marie Curie Intra-European Fellowship within the 6th European Community Framework Programme. We also thank The Spanish “Ministerio de educación y ciencia” for a postdoctoral fellowship.

Supporting Information Available: Cartesian coordinates of all the structures calculated and 3D representations of these structures. This material is available free of charge via the Internet at <http://pubs.acs.org>.

JO702088C